

Experimental evaluation of a full-color compact lensless holographic display

Michał Makowski,* Maciej Sypek, Izabela Ducin, Agnieszka Fajst, Andrzej Siemion, Jarosław Suszek and Andrzej Kolodziejczyk

Faculty of Physics, Warsaw University of Technology, 75 Koszykowa, 00-662 Warsaw, Poland

*michal.makowski@if.pw.edu.pl

Abstract: An iterative phase retrieval method for a lensless color holographic display using a single light modulator is experimentally validated. The technique involves iterative calculation of a three-plane synthetic hologram which is displayed on a SLM simultaneously lit with three laser beams providing an RGB illumination. Static and animated two-dimensional flicker-free full color images are reconstructed at a fixed position and captured using a high resolution CMOS sensor. The image finesse, color fidelity, contrast ratio and influence of speckles are evaluated and compared with other techniques of holographic color image encoding. The results indicate the technique superior in a case of full-color real-life pictures which are correctly displayed by this ultra-compact and simple projection setup.

©2009 Optical Society of America

OCIS codes: (090.1705) Color holography; (090.1760) Computer holography; (090.2870) Holographic display.

References and links

1. A. W. Lohmann, "Scaling laws for lens systems," *Appl. Opt.* **28**(23), 4996–4998 (1989).
 2. K. Hamanaka, and H. Koshi, "An artificial compound eye using a microlens array and its application to scale invariant processing," *Opt. Rev.* **3**(4), 264–268 (1996).
 3. J. Duparré, P. Schreiber, A. Matthes, E. Pshenay-Severin, A. Bräuer, A. Tünnermann, R. Völkel, M. Eisner, and T. Scharf, "Microoptical telescope compound eye," *Opt. Express* **13**(3), 889–903 (2005).
 4. R. Shogenji, Y. Kitamura, K. Yamada, S. Miyatake, and J. Tanida, "Multispectral imaging using compact compound optics," *Opt. Express* **12**(8), 1643–1655 (2004).
 5. M. Makowski, M. Sypek, and A. Kolodziejczyk, "Colorful reconstructions from a thin multi-plane phase hologram," *Opt. Express* **16**(15), 11618–11623 (2008).
 6. M. Makowski, M. Sypek, A. Kolodziejczyk, G. Mikula, and J. Suszek, "Iterative design of multi-plane holograms: experiments and applications," *Opt. Eng.* **46**(4), 045802 (2007).
 7. M. Makowski, M. Sypek, A. Kolodziejczyk, and G. Mikula, "Three-plane phase-only computer hologram generated with iterative Fresnel algorithm," *Opt. Eng.* **44**(12), 125805 (2005).
 8. R. W. Gerchberg, and W. O. Saxton, "A practical algorithm for the determination of phase from image and diffraction plane pictures," *Optik (Stuttg.)* **35**, 237–246 (1972).
 9. R. Dorsch, A. Lohmann, and S. Sinzinger, "Fresnel ping-pong algorithm for two-plane computer-generated hologram display," *Appl. Opt.* **33**(5), 869–875 (1994).
 10. T. Haist, M. Schonleber, and H. J. Tiziani, "Computer-generated holograms from 3D-objects written on twisted-nematic liquid crystal displays," *Opt. Commun.* **140**(4-6), 299–308 (1997).
 11. G. Sinclair, J. Leach, P. Jordan, G. Gibson, E. Yao, Z. J. Laczik, M. J. Padgett, and J. Courtial, "Interactive application in holographic optical tweezers of a multi-plane Gerchberg-Saxton algorithm for three-dimensional light shaping," *Opt. Express* **12**(8), 1665–1670 (2004).
 12. M. Sypek, "Light propagation in the Fresnel region: new numerical approach," *Opt. Commun.* **116**(1-3), 43–48 (1995).
 13. K. M. Johnson, M. Armstrong, L. Hesselink, and J. W. Goodman, "Multiple multiple-exposure hologram," *Appl. Opt.* **24**(24), 4467–4472 (1985).
 14. J. Suszek, M. Makowski, M. Sypek, A. Siemion, and A. Kolodziejczyk, "Angle-dependent encoding of multiple asymmetric symbols in a binary phase hologram with a spatial segmentation," *Appl. Opt.* **48**(2), 270–275 (2009).
 15. J. Xia, and H. Yin, "Three-dimensional light modulation using phase-only spatial light modulator," *Opt. Eng.* **48**(2), 020502 (2009).
-

1. Motivation and the display technique

The enduring miniaturization of handheld optical devices has encountered the fundamental problem of a diffraction limit when smaller and smaller lenses are used [1]. Especially in the field of micro-projectors it is difficult to achieve a fine bright color image with low aperture optics. The usual remedy for the limitations of the volume optics is the biologically inspired artificial compound optics [2–4], diffractive optics and holography. The first experimental demonstration of a lensless ultra-compact holographic projection technique which could potentially be applied to micro-projection is described in this paper. The main principle of the utilized method lies in the iterative calculation of a synthetic Fresnel hologram with three object planes each corresponding to a different color component obtained from a particular photograph [5–7]. The iterative phase retrieval itself is based on a classic Gerchberg-Saxton algorithm [8], modified by Lohmann et al. [9]. A similar method has been introduced by Haist et al. [10] and used for optical trapping by Sinclair et al. [11]. In our approach a single iteration starts in the object plane f_R with a random phase and an amplitude of the red component. The wavefront is then propagated to the second object plane f_G , where an amplitude of the green component is enforced without changing the phase. After a propagation to the closest object plane f_B an amplitude of the blue component is applied with phase left unchanged. Then the field is propagated to the hologram plane. There an amplitude equalization is done, which ensures a phase-only hologram in every iteration. The wavefront is propagated back to the object plane f_R . This loop is repeated a predefined number of times which leaves us with a phase distribution of an optimized three-plane Fresnel hologram. The object planes are designed at such distances f_R, f_G, f_B from the hologram which ensure the appearance of a color image at a fixed plane due to the chromatic dispersion of the holographic structure. In this work a base distance of 200 mm was chosen, which is potentially suitable for handheld projectors. When an iterated phase pattern of a three plane hologram is displayed on a spatial light modulator illuminated with a plane wave of $\lambda=632.8$ nm, three images are reconstructed at distances: $f_B=154$ mm, $f_G=168$ mm and $f_R=200$ mm. When the illuminating light is replaced with a plane wave of $\lambda=532$ nm, the obtained images are located at rescaled distances: 185 mm, 200 mm and 238 mm.

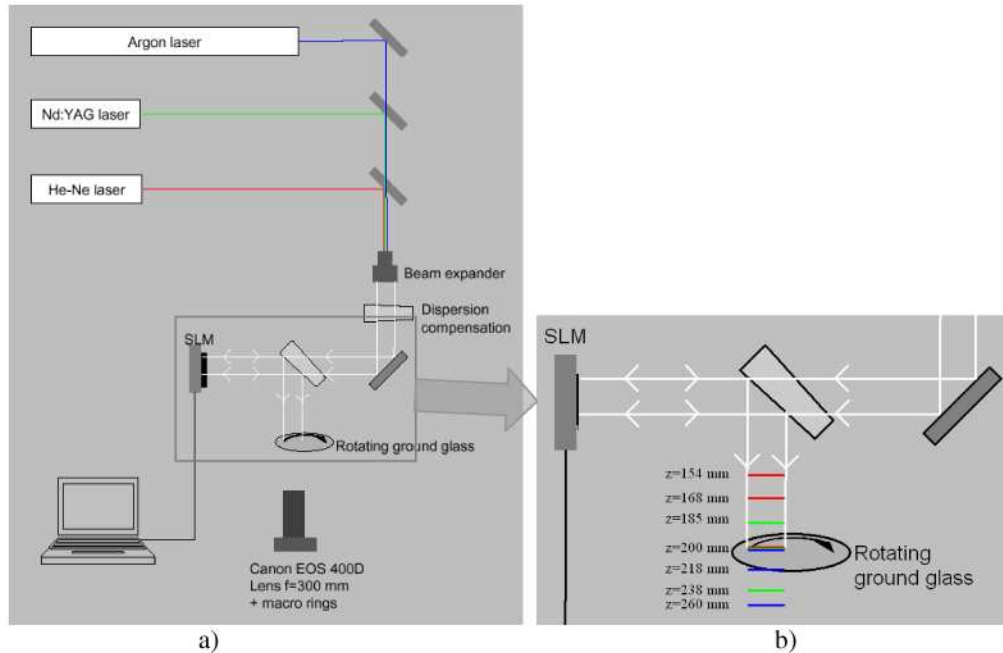


Fig. 1. a) An ideal scheme of the experimental setup; b) magnification of the marked area showing the locations of all reconstructed object planes with illumination from three beams.

In the last case when we used $\lambda=428$ nm, the distances were as follows: 200 mm; 218 mm and 260 mm. Therefore when we simultaneously illuminate the SLM with three beams, nine images are formed as seen in Fig. 1(b) and three of them are overlapped at a distance of 200 mm on a rotating ground glass, giving a color image. The mentioned distances f_R , f_G and f_B satisfy the Eq. (1), where λ_R , λ_G and λ_B are the wavelengths of red, green and blue laser beams, respectively.

$$f_G : f_R = \lambda_B : \lambda_G, f_B : f_R = \lambda_B : \lambda_R, f_B : f_G = \lambda_G : \lambda_R \quad (1)$$

The rotation of the ground glass eliminates the influence of the matt plate grooves on the photographs. Note that all color components are displayed at the same time, therefore the image is very stable in comparison with time sequential RGB displays, where a flicker or a rainbow effect is present. In the optical setup three RGB laser beams are coupled into a beam expander forming three plane waves which illuminate the spatial light modulator (Holoeye Pluto VIS, pixel pitch 8 μm , resolution: 1920 by 1080, 256 phase modulation levels). The modulated field is reflected through the semi-transparent mirror and reaches the rotating ground glass. An additional transparent prism-shaped element was added in order to compensate a misalignment of three color beams introduced by a refraction on the other prism-shaped mirror placed next to the SLM. The intensity distribution is photographed through the matt plate using a Canon EOS 400D digital camera, equipped with a CMOS sensor with pixel pitch of 5.7 μm and resolution of 3888 by 2592 pixels. Macro rings were necessary to achieve sharp images of the ground glass with a $f=300$ mm zoom objective. Fresnel hologram was calculated on a matrix of 2048 by 1024 points with a sampling of 8 μm . All propagations were numerically calculated using the modified convolution method [12]. This method was chosen because of its high speed, lack of pixel resampling and the longest range of properly calculated propagation distances. The input field is transformed using the FFT routine. Then it is multiplied by a complex factor dependant on the propagation distance. Finally, a reverse FFT transform returns the propagated diffractive field.

2. Alternative color encoding techniques

The proposed method has been experimentally compared with known techniques of encoding a color image into a single thin hologram, i.e. multi-exposure and surface segmentation. For both methods, the same set of input bitmaps was used. Three separate holograms of components R, G and B were calculated using a classic Gerchberg-Saxton algorithm in 100 iterations. For the multi-exposure method, the obtained phase distributions were numerically added one to another giving the final hologram, which is a numerical equivalent of a multiple exposure of a holographic plate [13]. Hence hologram of each component occupies the whole area of the SLM but has a decreased depth of phase modulation. In the surface segmentation method the three phase distributions were first multiplied by amplitude masks, shown in Fig. 2 and then added one to another. In this case hologram of each component occupies only one third of the SLM area, but with a full available depth of phase modulation. The same segmentation technique was used in our previous paper [14].

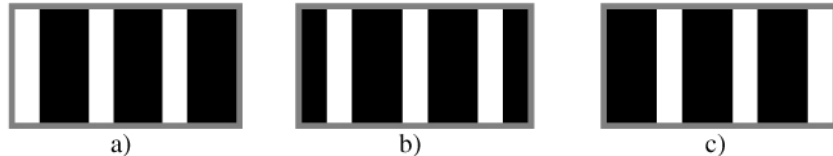


Fig. 2. Amplitude masks used in surface segmentation experiment for: a) red; b) green; c) blue component.

3. Experimental results

The images obtained from numerical simulations and different experiments are gathered in Fig. 4. The column “Input RGB image” contains the input bitmaps that were split into RGB

components and used in the calculation of a hologram. The column “Numerical reconstruction” shows the results of three separate numerical reconstructions of the obtained iterated holograms using the three wavelengths λ_R , λ_G and λ_B . Three monochromatic images were combined into a color image using GIMP. The contrast in the numerical reconstructions is inevitably lower in comparison with input bitmaps [7]. The decreased contrast is counterbalanced by a proper color reproduction.

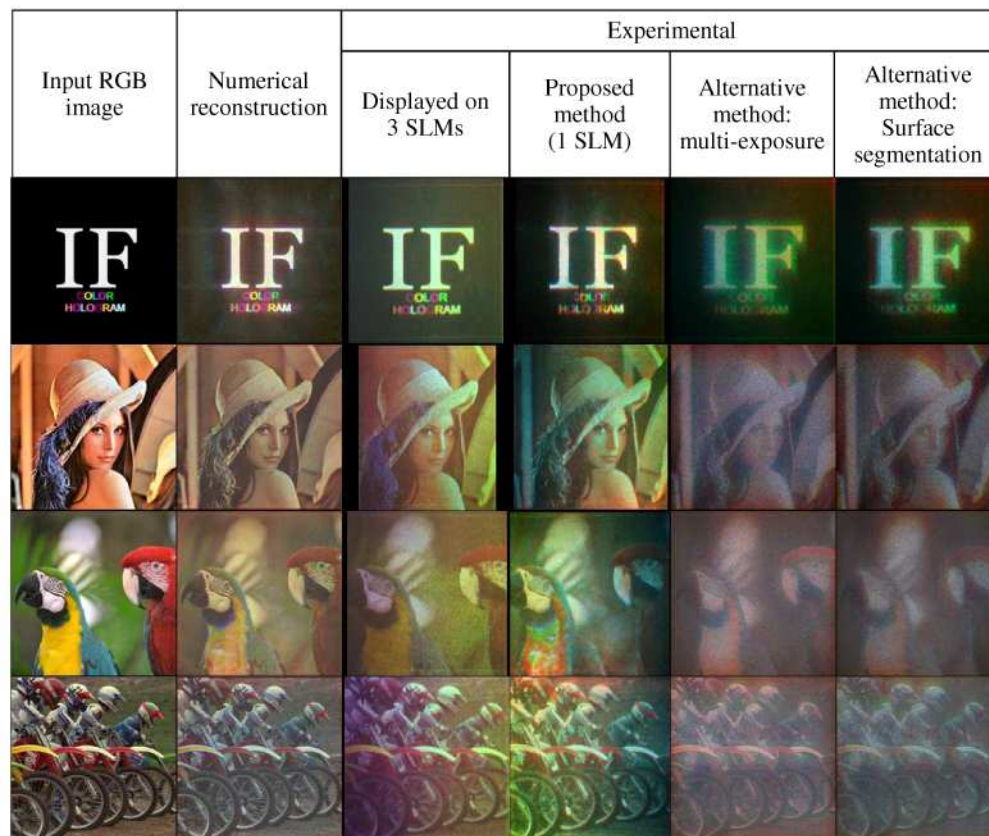


Fig. 4. The results of numerical and experimental reconstructions of color images for projection distance of 200 mm.

The next column, “Displayed on 3 SLMs”, shows the experimental realization of image reconstruction as if we could use 3 SLMs at the same time. This part was carried out by displaying three iterated one-plane holograms one after another, each illuminated by a laser beam with the wavelength λ_R , λ_G and λ_B , respectively. Then the three obtained experimental pictures were combined in GIMP in order to achieve a color image. The image finesse is excellent, nevertheless using three light modulators violates the main constraint of our concept: compactness and simplicity. The next column, “Proposed method”, contains images obtained from the experimental reconstructions on a single SLM by the use of our method. One can easily notice a good color reproduction in a case of smooth “real-life” pictures (rows 2-4) and slightly worse for the sharp image in the first row. Please note a fine agreement with the numerical predictions, shown in the second column. The results of the multi-exposure method shown in the next column exhibit a better color agreement for the “IF” image and a significantly lower contrast ratio that destroys the clarity. Additionally, one can notice a color cast surrounding objects on the images, which is typical for a superposition of one-plane holograms. Our iterative algorithm provides a three-plane hologram reconstructing the assumed images with a suppressed stray diffractive field in the vicinity of the object planes.

Therefore such a color cast is not visible, which is a major improvement. In the case of surface segmentation technique the highly visible color cast is asymmetric due to the shape of the used segmentation function. All the presented bitmaps are shown without any processing except for rotating and shrinking by 50% in width due to the fact that input images were horizontally stretched by 200% to occupy the whole area of the SLM. The numerical assessment of the image quality obtained from all three methods is shown in Table 1.

Table 1. Numerical comparison of the image quality using the mentioned four methods.

	3 SLM	Proposed method	Multi-exposure	Surface segmentation
Contrast ratio	5.3:1	3.3:1	1.5:1	1.9:1
Noise rate in bright/dark region	5.7% 11.4%	5.6% 12.3%	9.4% 14.2%	8.1% 16.9%

The contrast ratio was calculated as the average intensity in the bright test region divided by the average intensity in the dark test region, shown in Fig. 5. The noise rate was calculated as a standard deviation of the intensity divided by an average intensity in the test region. As seen in Table 1, the proposed method provides approximately two times higher contrast and approximately 56% lower noise ratio compared to the alternative methods under the same test conditions. Please note that the numerical assessment was only conducted on the sharp “IF” test image. Clearly, our method provides better results in the case of smooth test images (“Lena”, “Parrots” and “Speed racers”), although it is difficult to confirm that using statistics.

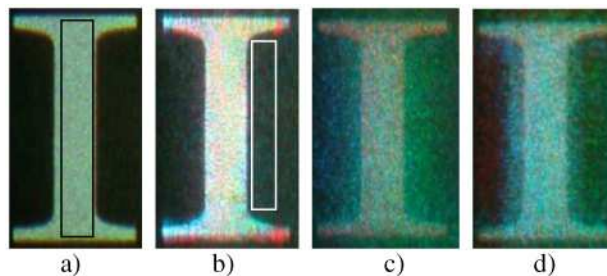


Fig. 5. Magnification of reconstructed images: a) 3 SLMs; b) proposed method; c) multi-exposure; d) surface segmentation. The “bright” test region is marked in black, the “dark” test region is marked in white.

Our method provides a color image by a superposition of three RGB component images on a screen. Nevertheless the other six reconstructed images are still present in different planes along the optical axis, which is illustrated in Fig. 1 and is recorded in Fig. 6(c) (Media 2).

To summarize, the achieved color reproduction and synchronization is correct. Any notable color smudges, as seen in Fig. 6(b), are caused only by imperfections of the alignment of laser beams into a beam expander. The gray levels of the SLM were optimized to achieve a 2π phase shift for $\lambda=632.8$ nm. A smaller modulation depth for green and blue beams was partly compensated by increasing their intensity. This fact combined with a 87% fill factor of the SLM caused an obstructing non-diffracted rectangular field visible in all the obtained photographs. That field inevitably decreases the contrast ratio. This issue could be overcome by the off-axis holography, but then severe misalignments in color components would be hard to suppress. This is the reason why we mainly present images with approximately the same pixel number as the phase array displayed on the SLM, i.e. 2048 by 1024 against 1920 by 1080. Larger images always exhibit non-diffracted field, as visible in Fig. 6. Additionally, since the large hologram is reconstructed from its relatively small fragment of 1920 by 1080 points, some negative effects occur. Speckles become larger and the depth of field increases thus causing the image planes to be less localized and therefore the color saturation is worse. Moreover, the large reconstructed image overlap with images from higher orders of

diffraction, as visible in Fig. 6(d). These are the reasons why increasing the size of the calculation array to achieve a large image is not the optimal concept.

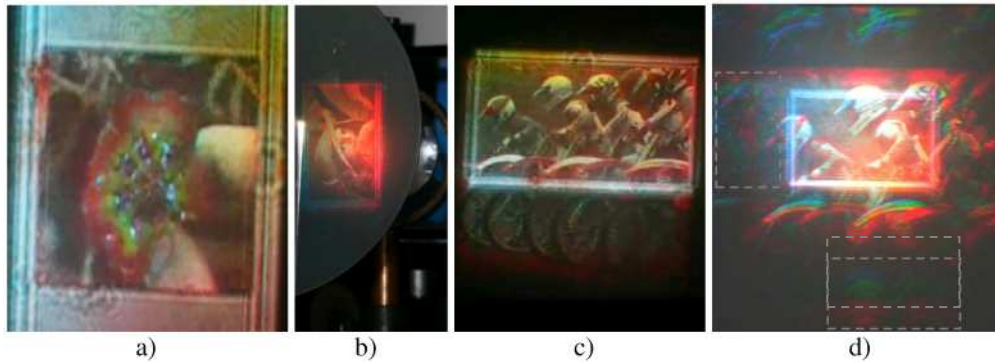


Fig. 6. Reconstruction of holograms designed on an array of: a) 1024 by 1024 ([Media 1](#) showing animations); b) 2048 by 1024; c) 2048 by 2048 ([Media 2](#) showing the diffractive field along the optical axis while approaching the SLM); d) 4096 by 4096 points. The non-diffracted field is visible and the presence of higher diffraction orders are marked in (d).

The presented experiment was also conducted for different base distances. Figure 7 shows the results of reconstruction of the same test image calculated on the array of 4096 by 4096 points for different projection ranges. Similar result were achieved for the array of 1024 by 1024 points. Larger distances introduce severe speckles in the obtained photographs, therefore the imaging distance is one of the limitations of the method, at least when using an SLM.



Fig. 7. Reconstruction quality for base projection distances: 500 mm; 700 mm and 1000 mm.

4. Conclusions and outlook

We have presented an experimental proof of a usefulness of our color lensless holographic display technique. The main features are a small and simple lensless optical setup, a use of only one light modulator and a flicker-free full-color image. Promising results were achieved at short working distances with various test images. The method is still under research not only by our group [15]. The quality of the obtained images seems to be limited mostly by the computational power and the used hardware, namely the pixel pitch and the fill factor of the light modulator. The important advantage of the utilized Fresnel diffuse hologram is the resistance of the output image to obstacles like dead pixels, dust, fingerprints or other obstruction on the large surface of the active area of the modulator. The future research will cover the optimization of calculation speed in order to achieve a real-time holographic encoding on a standard PC workstation. A preview of animated projection was recorded in the optical setup from pre-calculated phase distributions sequentially displayed on the SLM, see Fig. 6(a) ([Media 1](#)). Additionally, our aim will be to introduce a numeric way of enlarging the output images other than simply enlarging the hologram calculation matrix, which is extremely time-consuming.

Acknowledgements

The authors would like to thank HOLOEYE Photonics AG for a valuable support. This work has been supported by the European Union in the framework of European Social Fund through the Warsaw University of Technology Development Programme.